Physics Based Modelling of H-mode and Advanced Tokamak Scenarios for FAST: Analysis of the Role of Rotation in Predicting Core Transport in Future Machines

G.Calabrò 1), P.Mantica 2), B.Baiocchi 2),3), L.Lauro-Taroni 4),5), O.Asunta 6), M.Baruzzo 5), A.Cardinali 1), G.Corrigan 7), F.Crisanti 1), D.Farina 2), L.Figini 2), G.Giruzzi 8), F.Imbeaux 8), T.Johnson 9), M.Marinucci 1), V.Parail 7), A.Salmi 6), M.Schneider 8), M.Valisa 5)

1) Associazione Euratom-ENEA sulla Fusione, C.P. 65-I-00044-Frascati, Rome, Italy
2) Istituto di Fisica del Plasma 'P.Caldirola', Associazione Euratom-ENEA-CNR, Milano, Italy
3) Università degli Studi di Milano, Milano, Italy
4) New College, Oxford OX1 3BN, UK
5) Consorzio RFX, ENEA-Euratom Association, Padua, Italy
6) Association EURATOM-Tekes, Aalto University, Department of Applied Physics, Finland
7) Euratom/CCFE Association, Culham Science Centre, Abingdon, OX14 3DB, UK
8) CEA, IRFM, F-13108 Saint Paul Lez Durance, France
9) Association EURATOM-VR, Fusion Plasma Physics, EES, KTH, Stockholm, Sweden

E-mail contact of main author: giuseppe.calabro@enea.it

Abstract. The Fusion Advanced Study Torus (FAST) has been proposed as a possible European ITER satellite. This paper presents advanced core transport modeling work in order to predict FAST operational scenarios by combining existing predictive models and most recent transport experimental results from various devices, in particular JET. A special attention has been paid to the role of rotation, which appears an essential ingredient to achieve improved core ion confinement. Rotation is modeled by assuming a turbulence driven inward momentum pinch that allows for peaked profiles even in the presence of peripheral torque sources such as due to edge intrinsic rotation or NNBI at high plasma density. The impact of rotation on plasma performance has been evaluated either according to existing transport models or according to recent JET results on ion stiffness mitigation in presence of rotation and low magnetic shear. 7.5 T / 6.5 MA standard H-modes with 30 MW ICRH, or 20 MW ICRH and 10 MW NNBI, or 15 MW ICRH and 15 MW ECRH have been simulated. 3.5 T / 2 MA fully inductive AT scenarios have also been simulated, with 4 MW LH and 30 MW ICRH. All scenarios have been simulated using different transport models, either theory based or semi-empirical making use of recent JET experimental findings, and results critically assessed. The work has provided a sound scientific basis for the predictions of FAST performances and a range of scenarios for specific numerical studies of the role that FAST could play in investigating burning plasma physics as an ITER satellite.

1.Introduction

The Fusion Advanced Study Torus (FAST) has been proposed as a possible European ITER satellite [1] providing plasma conditions for integrated studies of plasma–wall interaction, burning plasma physics, ITER relevant operational issues and steady-state scenarios. Predicting performance and scenarios in future fusion devices beyond the level of 0D scaling laws is a challenging task. On one hand we do not yet have at disposal fully validated core and edge predictive transport models, on the other hand assuming 1D profile conservation starting from data in existing machines and using dimensionless parameter scaling is at least partially hindered by expected differences between present and future machines, such as in plasma rotation, amount of electron heating and impurity concentrations. In this situation, the predictive activity must wisely combine both theory based simulations and empirically based considerations, with the strongest possible link to experimental results in existing devices.
In this spirit, the initial study of FAST scenarios [2] has been refined by considering both the predictions of several physics based or semi-empirical transport models and the recent transport experimental results on devices such as JET, DIII-D and C-MOD. H-mode and Advanced Tokamak are the investigated FAST scenarios. For H-mode the first analyzed (reference) case is characterized by B_t=7.5 T and I_p=6.5 MA. Heating power equal to 30 MW is provided by the ICRH system at 73 MHz in (^{3}He)-D minority scheme. B_t=6 T and I_p=5.5 MA characterize the second case, where the heating power is given by 15 MW, provided by the ICRH system at 58 MHz in (^{3}He)-D minority, and 15 MW, provided by the ECRH system

(170 GHz, 1st Harmonic O-mode from LFS). Third, the effect of replacing 10 MW of ICRH power with 10 MW of NNBI power (with beam energy of 700 keV) in the H-mode reference scenario is investigated. Last, for the Advanced Tokamak scenario B_t=3.5 T and I_p=2 MA are the chosen parameters. The heating power is 30 MW, either provided fully by the ICRH system at 35 MHz in (^{3}He)-D minority, or by 20 MW ICRH and 10 MW NNBI, plus 4 MW provided by the LH at 5 GHz, n||=2.3.

2. Simulations set-up

The simulations have been carried out using the JETTO code ([3], part of the JAMS JET suite of integrated codes). For ICRH heating profiles we have either used the PION code [4] called self-consistenly by JETTO or the TORIC code [5] which is run outside JETTO and requires a few iterations. Good match between the RF deposition predicted by the two codes is shown in Fig. 1 for the case with n_{3He}/n_e=3%.

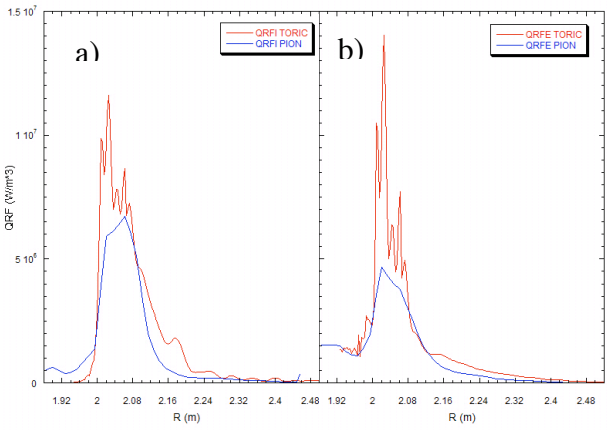

FIG.1. ICRH deposition profiles for ions (a) and electrons (b) with red lines for TORIC and blue lines for PION (7.5T, 73 MHz, n_{3He}/n_e=3%).

The ECRH heating profiles have been provided by the GRAY code [6], which is also outside the JAMS suite and required iterations with JETTO. For AT scenarios FRTC [7], within the JAMS suite, has been used to calculate LH heating and current drive profiles.

The NNBI power and torque profiles have been computed using the orbit following ASCOT code [8] called self-consistently by JETTO or the NEMO [9] and SPOT [10] codes which are run outside JETTO.

Different core transport models have been used: first principle models (Weiland [11] and GLF23 [12]) and semi-empirical models (mixed Bohm-gyroBohm (BgB) [13] and Critical Gradient Model [14]). In the CGM simulations the electron threshold has been calculated after [11] and ion threshold after [15] whilst the stiffness coefficients have been chosen following the results of recent transport experiments on JET [16,17,18], i.e. χ_{se}~1 for electrons and χ_{si}~2-4 for ions, which implies rather high stiffness for both heat transport channels. The pedestal values have been chosen in accordance with pedestal scaling as the modelling work has focused on the core transport issues. All the simulations have been made with evolving current, ion and electron temperatures. For the H-mode scenario the density profile has been in first instance assigned with rather flat shape according to typical H-mode density profiles, in second instance calculated with first-principle models, resulting in significant peaking due to the low collisionality. When the effect of rotation is considered, the toroidal momentum transport equation is also solved. According to recent theory developments [19], the assumptions of Prandtl number Pr= χ_φ/χ_i =1 and pinch number Rv_φ/χ_φ~4 are made, where v_φ is a turbulence driven inward momentum pinch. These assumptions have also been confirmed experimentally in JET and other devices [20,21,22]. In all the following figures, the radial coordinate is the square root of the normalized toroidal magnetic flux, indicated as rhotn.

3. Reference H-mode scenario with 30 MW ICRH

In Fig. 2 the ion and electron temperature profiles together with the assigned density profile for 30 MW ICRH H-mode are shown using different transport models. It is evident that, whilst for electrons the range of predicted temperatures is not large, although the BgB model gives much broader T_e profiles than all other models, for ions there is a wide range of predictions, up to a factor 2 in central T_i. A choice must then be made amongst the different models

to select the most reliable prediction, since it is not granted that all the above models work well in the domain of high B_T machines, as they have commonly been validated against data of medium-size, lower B_T machines. We tend to attach better reliability to the predictions of GLF23 which has the broadest physics basis and to CGM which is derived directly from JET experimental data, and which turns out to agree to good extent with GLF23. Therefore we would retain as most reliable prediction, for the FAST reference H-mode scenario with 30 MW ICRH, values of T_{i0}~13 keV, T_{e0}~15 keV with a density n_{e0}~2.4 10^{20} m^{-3} and a confinement time τ~0.4 s, yielding $n_{e0}T_{i0}\tau \sim 1.5\ 10^{21}$ keVs/m^3.

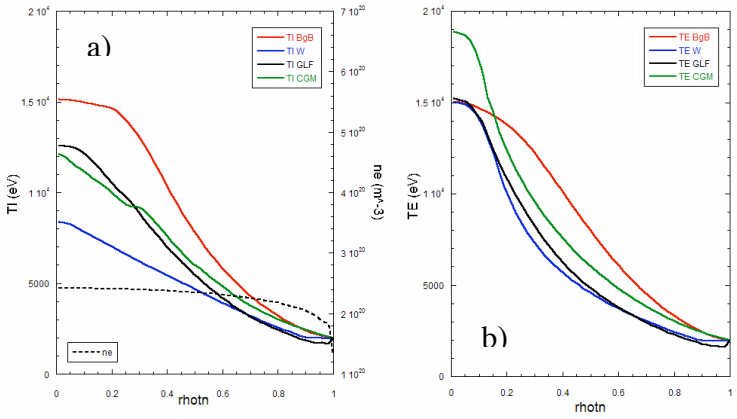

FIG.2. Ion (a) and electron (b) temperature profiles for 7.5T reference H-mode scenario, 30 MW ICRH calculated with PION, using different transport models: red profiles are for BgB, blue for Weiland, black for GLF 23 and green for CGM. The assigned density profile is shown in (a) with dotted line.

In order to obtain a more physics based simulation, also the density profile has been calculated consistently by the different models (BgB, Weiland, GLF23). Temperature and density profiles obtained using different transport models are shown in Fig.3. Good agreement between the 3 different models has been found in predicting a rather peaked n_e profile, which makes conditions easier from the point of view of plasma-wall interaction, still retaining high central n_e values. The simulations with GLF23 corresponds to T_{i0}~11 keV, T_{e0}~13 keV with a density n_{e0}~3.3 10^{20} m^{-3} and a confinement time τ~0.5 s, yielding $n_{e0}T_{i0}\tau$ ~1.7 10^{21} keVs/m^3.

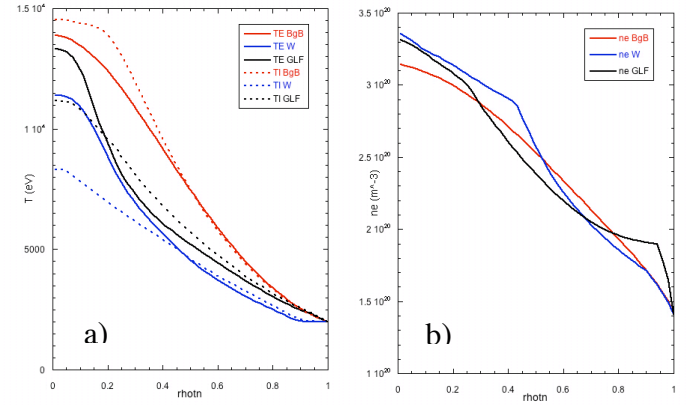

FIG. 3. Ion and electron temperature profiles (a) and calculated density profiles (b) for 7.5 T reference H-mode scenario, 30 MW ICRH calculated with PION, using different transport models: Bohm-gyroBohm in red, Weiland in blue, GLF23 in black.

4. H-mode scenario with 15 MW ICRH and 15 MW ECRH

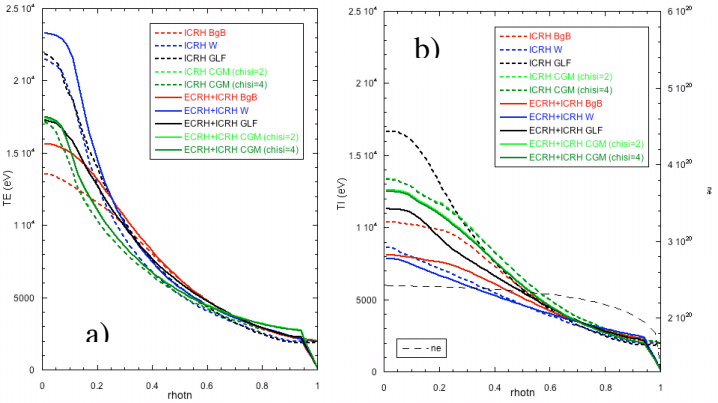

FIG.4. Ion and electron temperature and assigned density profiles for the case of 6 T H-mode with ICRH +ECRH (full line) and full ICRH (dotted line). Red lines are for old BgB, blue for Weiland, black for GLF23 and green for CGM. ICRH is calculated with TORIC.

Substituting 15 MW of ICRH with 15 MW of ECRH power gives the temperature profiles shown in Fig. 4, where they are directly compared to those with 30 MW ICRH. Differently from Fig. 2, for both cases ICRH profiles are provided by TORIC, and the BgB model was used in an older version. The substitution of 15 MW ICRH with 15 MW ECRH is not beneficial from the point of view of confinement, although it alleviates the issue of high impurity influx from ICRH antenna. In fact, increased electron heating and decreased ion heating, together with the decrease in ITG threshold associated to higher T_e/T_i values and the high electron stiffness, yield colder ions and not significantly hotter electrons than the full ICRH case. Therefore we have proceeded with the analysis focusing on the 30 MW ICRH H-mode, and investigating in detail the effect of plasma rotation.

5. H-mode scenario simulations including the effect of rotation

Finally, also the role of toroidal rotation has been taken into account. From recent experimental results it seems to have a key role in achieving improved ion core confinement [16,17,18,23,24], not only through the well-known threshold up-shift, but through a significant reduction of the ion stiffness. Such ion core confinement improvement is an essential ingredient for obtaining steady-state scenarios with a core region of enhanced pressure gradient and associated bootstrap current. The rotation has been included in the simulations by self-consistently modelling also the momentum transport with the physical assumptions described in Sect.2. Two sources of rotation have been considered. First, the edge driven intrinsic rotation, which, due to the inward pinch, can be transported into the plasma core. This intrinsic rotation is a well known observation in tokamaks [25,26], but a quantitative understanding of the phenomenon is still lacking, therefore extrapolation to non-existing devices is to be taken with care. Second, the core torque due to 10 MW NNBI, which allows a safer prediction through the ASCOT code.

5.1 H-mode scenario with 30 MW ICRH and intrinsic rotation

Given the present lack of understanding and theory-based predictive capability on intrinsic rotation, we have assumed for FAST an edge rotation value ω_φ=30 krad/s, as provided by the scaling in [25], although such scaling has recently been questioned on the basis of new JET experimental evidence [26]. However, since high values of intrinsic rotation are measured in C-MOD, a high field compact machine conceptually similar to FAST, it may be still legitimate to assume for FAST an edge rotation value as predicted by the existing C-MOD driven empirical scaling. No torque sources are included. Fig.5a shows the rotation profile obtained with the assumptions described above. A very significant rotation gradient is predicted. In or-

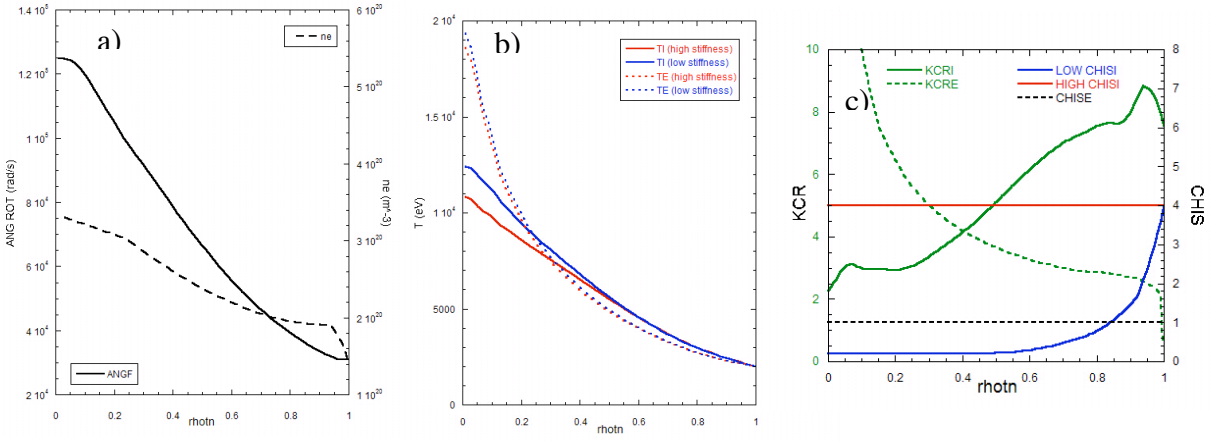

FIG. 5. Assigned peaked density and calculated rotation (a) and T_i, T_e (b) profiles for 7.5 T 30 MW ICRH H-mode scenario using Pr=1, Rv_φ/χ_φ~4 and edge intrinsic rotation for momentum transport and CGM for heat transport with low ion stiffness in the rotating case.(c)Threshold (kcr) and stiffness (chis) profiles for ions and electrons.

order to estimate the rotation impact on confinement we have not used first-principle models like Weiland or GLF23, which contain only the effect on threshold, but we have used the CGM model in which the stiffness value has been decreased in the centre as found in JET and discussed in [17,18]. The assumed profiles for threshold and stiffness are shown in Fig.5c. Whilst the threshold profiles are calculated using theory-based formulas, the stiffness profiles have been taken from JET results with/without rotation. Obviously this extrapolation is totally arbitrary, but we presently lack a theoretical model describing the effect of rotation on ion stiffness, which has been experimentally found much more significant than the threshold up-shift in JET. Fig.5b shows the impact on ions (electrons are unaffected by rotation). It is seen that in the H-mode scenario the impact of rotation is significant from ρ~0.5 to the centre. With the effect of the rotation the ion temperature increases by 1.5 keV.

5.2 H-mode scenario with 20 MW ICRH and rotation driven by 10 MW NNBI

Instead of an intrinsic source of rotation we can provide a sounder source of rotation introducing the NNBI power [27]. In particular 10 MW of RF heating have been replaced by 10 MW of NNBI. The NNBI power depositions, calculated by ASCOT, can be seen in Fig.6a and are peaked at the plasma centre, although a very significant fraction of power is deposited externally due to the high density. In fig. 6b the torques are presented. The collisional torque is the dominant one in the central region, whilst the JxB torque is dominant in the region ρ>0.5.

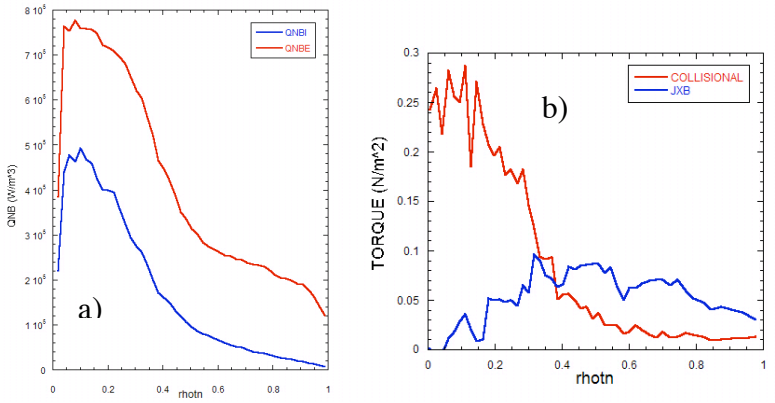

FIG. 6. NNBI power depositions (a) and torque (b) profiles calculated by ASCOT for 7.5 T 10 MW NNBI + 20 MW ICRH H-mode scenario using BgB for heat transport.

Fig.7 shows the rotation profiles obtained with 10 MW NNBI + 20 MW ICRH both in absence and in presence of an edge driven intrinsic rotation, compared with the cases at 30 MW ICRH. In all cases the momentum equation is solved using the diffusivity and pinch calculated as discussed in Sect.2. The heat transport is calculated using the BgB model with the ad hoc criterion that switches off turbulent transport in the region where a suitable combination of ExB flow shear and magnetic shear is reached [13]. This is of course a very rough model, which produces the same effect on transport (likely overestimated, if one compares with

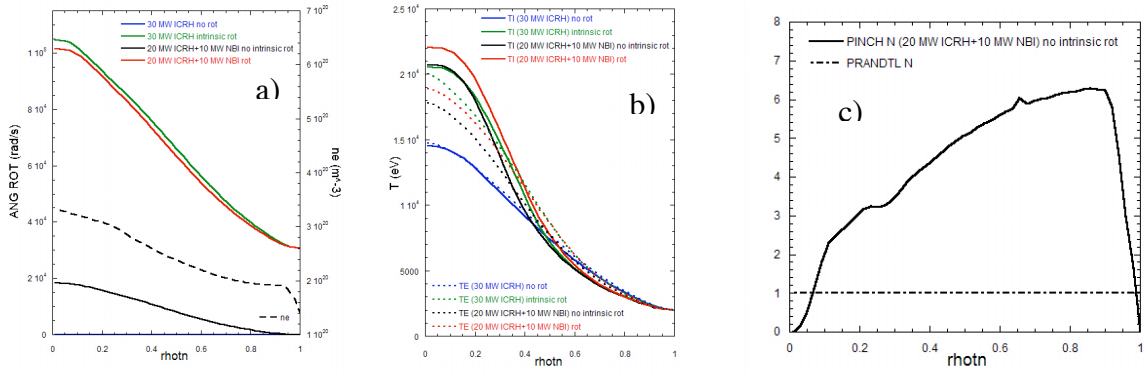

FIG. 7. Assigned peaked density and calculated rotation (a), T_i, T_e (b) profiles and Pinch and Prandtl numbers (c) for 7.5 T 30 MW ICRH (blue without and green with edge intrinsic rotation) and 20 MW ICRH + 10 MW NNBI (black without and red with edge intrinsic rotation) H-mode scenario using BgB for heat transport.

Fig.5b) for any rotation value that fulfils such criterion, irrespective of its value. One can see that the rotation induced by the NNBI, in the absence of intrinsic rotation, is already enough to produce stabilization with respect to the full ICRH non-rotating case, thereby peaking the temperature profiles significantly. Adding an edge intrinsic rotation under the assumptions described earlier clearly dominates on the effect on the NBI torque, but the temperature profiles do not peak further due to the model assumptions. It is important to remark however that the NNBI driven rotation is based on a sounder physics, and therefore would ensure in FAST a basic level of rotation, on top of which intrinsic rotation can further improve the attained rotation values.

6. H-mode extreme with 30 MW ICRH

In FAST, the extreme H-mode scenario requires 40 MW of external heating, supplied by negative neutral beam injection (NNBI - 10MW) and ion cyclotron resonance heating (ICRH-30MW), as discussed in [2,29]. The extreme H-mode is characterized by high magnetic field B=8.5T and high plasma current I_p=8MA for a discharge time duration of about 12s and peak density up to $5x10^{20}m^{-3}$. Here, preliminary numerical results obtained self-consistently by the transport code JETTO iteratively used with the external bi-dimensional full wave-quasi-linear solver (TORIC/SSFPQL) for only ICRH heating (30MW) in D plasma, are reported. The GLF23 transport model has been used in these simulations and the density is predicted, whilst rotation is not included. The ICRH frequency range $78\,MHz \le f_{ICRH} \le 82\,MHz$ has been considered to deal with an off-axis power deposition profile (ρ_{tor}=0.07-0.21), while the 1-3% ^{3}He dilution is chosen to optimize the minority-heating scheme efficiency [28]. In Fig. 8, the electron and ion temperature (a), and electron density (b), are shown at the flat-top of the discharge simulation.

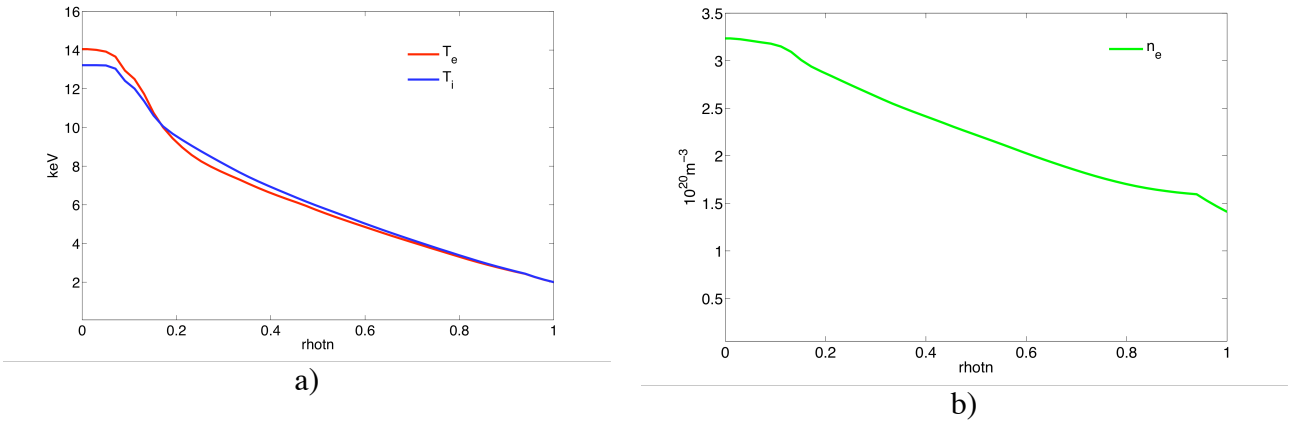

a) b)

FIG. 8. Ion and electron temperature profiles (a) and calculated density profiles (b) for 8.5 T extreme H-mode scenario, 30 MW ICRH calculated with TORIC, using the GLF23 transport model.

7. AT scenario simulations including the effect of rotation

The role of rotation is essential in AT scenarios, as it has been shown experimentally in several machines that the q profile alone is not sufficient to provide ion ITB formation. A test simulation of a 3.5 T AT scenario with 30 MW ICRH with reversed q has been performed using the BgB model. In the case with intrinsic rotation the ITB criterion embedded in the model is switched on, yielding ITB formation. This is compared with the case without rotation in Fig.9. A fully non-inductive pulse can be achieved with the intrinsic edge rotation, fully reversed q profile, and sustained ITB at ρ~0.6. Indicative values are T_{i0}~20 keV, T_{e0}~15 keV with a density n_{e0}~2 10^{20} m^{-3} and a confinement time τ~0.2 s, yielding a value $n_{e0}T_{i0}\tau$ ~8 10^{20} keVs/m^3. These parameters have to be regarded as overestimated due to the simplistic assumptions of the BgB model. Attempts to use GFL23 were unsuccessful due to numerical instabilities. As shown in Fig.7 for the H-mode scenario, also in AT scenario substituting 10

MW of ICRH with 10 MW of NNBI power does not make a significant difference to the performance within the assumptions of the BgB model. As remarked before, however, NNBI provides a more reliable source for toroidal rotation, which is an essential ingredient for achieving ITB formation.

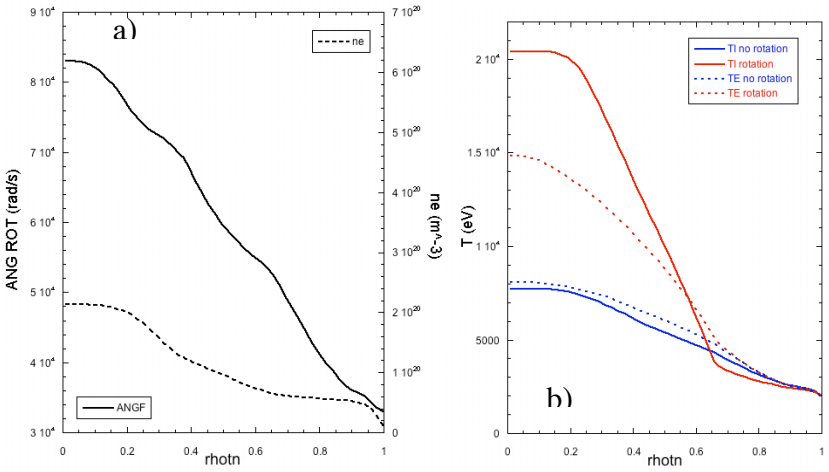

Fig. 9: Density and rotation profiles (a) and ion and electron temperatures without and with rotation (b) for a 3.5 T ICRH+LH AT scenario with reversed q profile. Rotation is driven by edge intrinsic rotation and momentum pinch. Bohm-gyroBohm is used for heat transport and TORIC for ICRH.

8. Conclusions

In conclusions, refined core transport modelling of FAST scenarios based on a careful combination of existing theory based models and latest experimental results from existing machines confirmed the expectation that FAST will be a valuable aid to ITER exploitation. The reference H-mode scenario performance has been assessed thoroughly, fully predicting T_e, T_i, n_e, and rotation, and evaluating the effect of rotation on thermal transport. The idea of lowering the amount of ICRH power by introducing an additional type of heating has been evaluated. ECRH does not seem advantageous, whilst NNBI offers various advantages, providing both fast particle energy in parallel direction and a safer basis for the existence of a beneficial toroidal rotation with respect to the mere intrinsic one. This will also allow to achieve fully non-inductive AT scenarios with ITB formation. The simulations provided a range of scenarios on which fast particle and burning plasma studies can be performed. Fig.9 shows TORIC calculations for the perpendicular beta of the fast ^{3}He ions (β_{hot}^{perp}) heated by 30 MW ICRH at ^{3}He=3% (peak power density on the minority species~15 MW/m^3) in the reference H-mode scenario, as a function of density and electron temperature. In the transport simulations presented above for the H-mode reference scenario, typical values at the ICRH deposition (ρ_{tor}~0.25) are T_e~8 keV, n_e~2.8 10^{19} m^{-3}, resulting in β_{hot}^{perp}~2%. These values are well in line with the needs for exciting meso-scale fluctuations with the same characteristics of those expected in reactor relevant conditions, as investigated in detail in [28]. Lowering the ^{3}He concentration results ultimately in a lower beta due to lower peak values of power density and lower minority density, although the fast ion energies increase. The extreme H-mode scenario is of interest also for fast particle studies, as it helps their confinement due to the high current, at the condition that plasma density is maintained low, as discussed in Sect.6 and in [28]. The corresponding values of the perpendicular temperature of the energetic tail and β_{hot}, in the optimized case of 82MHz and calculated by means of the anisotropic distribution function obtained by TORIC+SSFPQL are reported in [28]. β_{hot}reaches a peak ~ 4% for a deposition very close to the magnetic axis and ~ 1% for the more realistic case (78MHz) of absorption outside to the q=1 surface. These values are consistent with the request of accessing ITER-relevant conditions. The scenario flexibility available in FAST, as documented in this paper, is an important element for energetic particle physics studies.

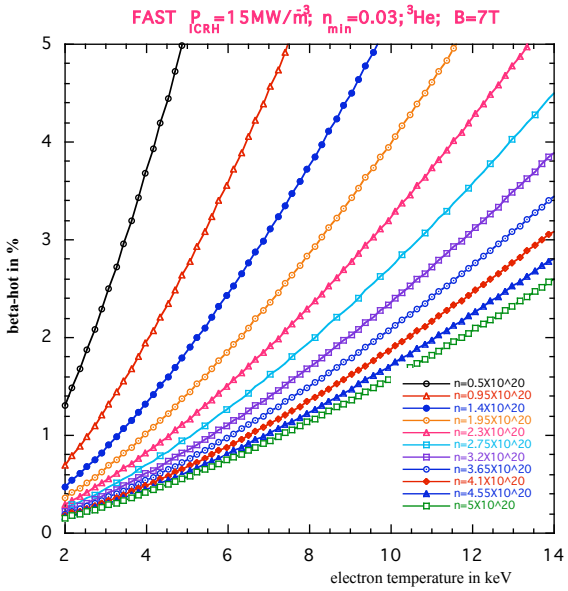

Fig. 9: Perpendicular beta of the fast particle component calculated by TORIC in reference H-mode scenario with 30 MW ICRH (~15MW/m^3 peak power density) at ^{3}He=3% as a function of T_e for different density values.

This work, supported by the European Communities under the contract of Association EURATOM/ ENEA-CNR, was carried out within the framework of EFDA. The views and opinions expressed herein do not necessarily reflect those of the European Commission.

References

[1] CARDINALI, A., et al., Nucl. Fusion **49** (2009) 095020
[2] CALABRÒ, G., et al., Nucl. Fusion **49** (2009) 055002
[3] CENACCHI, G. and TARONI, A., *JETTO: A free boundary plasma transport code (basic version) Rapporto ENEA RT/TIB 1988(5).*
[4] ERIKSSON, L-G, et al., Nucl. Fusion **33** (1993) 1037
[5] BRAMBILLA, M., Plasma Phys. Contr. Fusion **41** (1999) 1
[6] FARINA, D., "GRAY: a quasi-optical ray tracing code for electron cyclotron absorption and current drive in tokamaks", *IFP-CNR Internal Report FP* 05/1 and http://www.ifp.cnr.it/ publications/ 2005/FP05-01.pdf
[7] ESTERKIN, A.R. and PILIYA, A.D., Nucl. Fusion **36** (1996) 1501
[8] HEIKKINEN, J.A. and SIPILÄ , S.K., Phys. Plasmas **2** (1995) 3724
[9] SCHNEIDER M., *et al., to be submitted to Nucl. Fusion*
[10] SCHNEIDER M., et al., Plasma Phys. Control. Fusion **47** (2005) 2087
[11] WEILAND, J., *Collective Modes in Inhomogeneous Plasmas*, IOP (2000)
[12] WALTZ, R.E., et al., Phys. Plasmas **4**(1997) 2482
[13] ERBA, M., et al., Plasma Phys. Control. Fusion **39,** (1997) 261
[14] GARBET, X., et al., Plasma Phys. Contr. Fusion **46** (2004) 135
[15] GUO S. C and ROMANELLI, F., Phys. Fluids B 5, (1993) 520
[16] MANTICA, P., et al., Fusion Science and Technology **53** (2008) 1152
[17] MANTICA, P., et al., Phys. Rev. Lett. **102** (2009) 175002
[18] MANTICA, P., et al., EXC/9-2, this conference
[19] PEETERS, A.G.G., et al., OV/5-4, this conference
[20] MANTICA, P., et al., Phys. Plasmas, Sept 2010
[21] TALA, T., et al., EXC/3-1, this conference
[22] SOLOMON, W.M., et al., Nucl. Fusion **49** (2009) 085005
[23] DE VRIES, P., et al., Nucl. Fusion **49** (2009) 075007
[24] POLITZER, P.A., et al., Nucl. Fusion **48** (2008) 075001
[25] RICE, J., et al., Nucl. Fusion **47** (2007) 1618
[26] NAVE,M.F.F., et al.,in Proc.37th EPS Conference on Plasma Physics, Dublin, Ireland,(June 2010)
[27]BARUZZO,M.,et al.,in Proc.37th EPS Conference on Plasma Physics, Dublin, Ireland,(June 2010)
[28] CARDINALI, A., et al., THW/P7-04, this conference
[29] CRISANTI, F., et al., FTP/2-4, this conference